

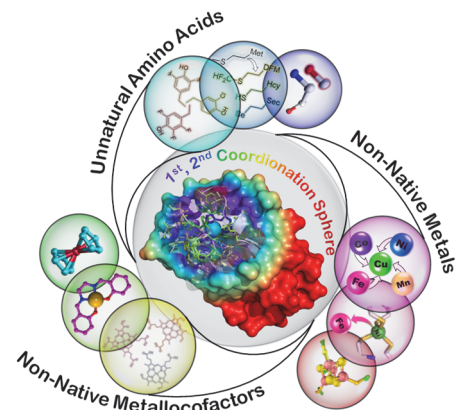
# Understanding and Modulating Metalloenzymes with Unnatural Amino Acids, Non-native Metal Ions, and Non-native Metallocofactors

EVAN N. MIRTS, AMBIKA BHAGI-DAMODARAN AND YI LU

*Department of Chemistry and Center for Biophysics and Quantitative Biology, University of Illinois at Urbana-Champaign, Urbana, IL 61801, USA*

## Conspectus

Metalloproteins set the gold standard for performing important functions, including catalyzing demanding reactions under mild conditions. Designing artificial metalloenzymes (ArMs) to catalyze abiological reactions has been a major endeavor for many years, but most ArMs' activities are far below those of native enzymes, making them unsuitable for most practical applications. A critical step to advance the field is to fundamentally understand what it takes to not only confer but also fine-tune ArM activities so they match native enzymes. Indeed, only once we can freely modulate ArM activity to rival (or surpass!) natural enzymes can the potential of ArMs be fully realized. A key to unlocking ArM potential is the observation that one metal primary coordination sphere (PCS) can display a range of functions and levels of activity, leading to the realization that secondary coordination sphere (SCS) interactions are critically important. However, SCS interactions are numerous, long-range, and weak, making them very difficult to reproduce in ArMs. Furthermore, natural enzymes are tied to a small set of biologically available functional moieties from canonical amino acids and the physiologically available metal ions and metallocofactors, severely limiting the chemical space available to probe and tune ArMs. In this Account, we summarize our group's use of unnatural amino acids (UAs) and non-native metal ions and metallocofactors to probe and modulate ArM functions. We incorporated isostructural UAs in a type 1 copper (T1Cu) protein azurin to provide conclusive evidence that the axial ligand hydrophobicity is a major determinant of T1Cu reduction potential ( $E^\circ$ ). We also probed the role of protein backbone interactions that cannot be altered by standard mutagenesis by replacing the peptide bond with an ester linkage. We used insight gained from these studies to tune the  $E^\circ$  of azurin across the entire physiological range, the broadest range ever achieved in a single metalloprotein. Introducing UA analogs of Tyr into ArM models of heme-copper oxidase (HCO) revealed a linear relationship between  $pK_a$ ,  $E^\circ$ , and activity. We have also substituted non-native hemes and non-native metal ions for their native equivalents in these models to resolve several issues that were intractable in native HCOs and the closely related nitric oxide reductases (NOR), such as their roles in modulating substrate affinity, ET rate, and activity. We have incorporated abiological cofactors such as ferrocene and Mn(salen) into azurin and myoglobin, respectively, to stabilize these inorganic and organometallic compounds in water, confer abiological functions, tune their  $E^\circ$  and activity through SCS interactions, and show that the approach to metallocofactor anchoring and orientation can tune enantioselectivity and alter function. Replacing Cu in azurin with non-native Fe or Ni can impart novel activities, such as superoxide reduction and C-C bond formation. While progress has been made, we have identified only a small fraction of the interactions that can be generally applied to ArMs to fine-tune their functions. Because SCS interactions are subtle and heavily interconnected, it has been difficult to characterize their effects quantitatively. It is vital to develop spectroscopic and computational techniques to detect and quantify their effects in both resting states and catalytic intermediates



## 1. Introduction

Metalloproteins perform challenging functions in nature, including transferring electrons across long distances and catalyzing demanding reactions with high regio- and stereoselectivity, and they accomplish them under ambient conditions in water. They have inspired many chemists and biochemists to design artificial metalloenzymes (ArMs) to mimic native enzymes,<sup>1,2</sup> with a major branch of this field focusing on abiological reactions. Despite significant progress over early models, most ArMs still display much lower activity than native enzymes. To advance this field, it is necessary to devote considerable effort toward understanding how enzyme structural features are responsible

for their high activity and selectivity and how to modulate these traits beyond their natural ranges for practical applications. Only once we can demonstrate the ability to control properties of metalloproteins at-will so they rival (or surpass!) natural enzymes will it be possible to realize the full potential of ArMs.

A fascinating feature of metalloproteins is that the same metal-binding site consisting of a conserved set of ligands coordinated to a metal ion in a characteristic geometry (defined as the primary coordination sphere, or PCS) can display a variety of electronic properties and perform many different functions in different metalloproteins. Nature accomplishes this amazing feat with multiple non-covalent and asymmetric interactions with residues in the second coordination sphere (SCS) and beyond, such as electrostatic and hydrophobic interactions, dipole moments, and hydrogen bonding. Harnessing this “trick” from nature is critical for designing synthetic models using organic molecules as ligands or ArMs with high activity toward abiological reactions. However, these myriad weak interactions can be extremely difficult to reproduce in synthetic catalysts, for which a ligand capable of providing the same degree of SCS control provided by a protein matrix would be prohibitively large and difficult to synthesize. Designing ArMs based natural protein scaffolds can overcome these limitations.

A major design barrier for ArM SCS control is that site-directed mutagenesis of one of the 20 canonical amino acids (AA) to another often changes multiple factors (e.g., steric and electronic properties) simultaneously. Replacing AAs with unnatural amino acid (UAA) isostructural analogs can deconvolute sterics from other factors. More importantly, UAAs introduce new functional groups to tune the ArM beyond natural enzymes. Similarly, replacing metal ions or metallcofactors (e.g., heme) found in native metalloproteins with non-native metal ions or metallcofactors has allowed exploration and modulation of metalloprotein properties in a much broader chemical space and made it possible to perform difficult reactions with ever-increasing efficiency.<sup>3</sup> In this Account we summarize how UAAs and non-native metals and metallcofactors have filled gaps in our understanding of the precise roles of native AAs, metals, and metallcofactors in protein functions, pushed the natural limits of protein-metal interactions, and modulated functions beyond the limits of natural metalloproteins.

## 2. Understanding and Modulating Biological Function with UAAs

Redox reactions are at the heart of many metalloprotein functions; therefore, reduction potential ( $E^{\circ'}$ ) of the metal center is a major determining factor of their activities. A prime example is type 1 copper (T1Cu) proteins, which contain a copper center coordinated by one Cys and two His residues in a trigonal plane. Even though all mononuclear T1Cu proteins contain the same PCS (Fig. 1A), the  $E^{\circ'}$  of the Cu(II)/Cu(I) couple can range from +180 to +800 mV<sup>4,5</sup> vs. standard hydrogen electrode (SHE); all  $E^{\circ'}$  values in this Account are reported against SHE. While  $E^{\circ'}$  of metal ions can be tuned by changing the PCS, this perturbs the redox couple reorganization energy, which in turn affects ET function. T1Cu proteins overcome this issue by relying on the SCS to tune  $E^{\circ'}$ , such as the weak axial ligand above the trigonal plane, typically Met or Gln (Fig. 1A). Though it is a weak Cu-ligand in most cases, the axial residue is considered SCS because non-coordinating residues such as Leu are found in some T1Cu, and mutating this residue modulates  $E^{\circ'}$  whether it coordinates Cu or not. Therefore, hydrophobicity of the axial ligand has been proposed to be a major determining factor for  $E^{\circ'}$ . However, the different axial ligands are not isostructural, so other complex effects cannot be ruled out. We investigated this question through isostructural UAAs that covered a wide range of functional moieties. For example, we used expressed protein ligation (EPL)<sup>6</sup> to replace Met121 in wild type azurin from *Pseudomonas aeruginosa* (WT-Az) with isostructural UAA analogs: difluoromethyl (DFM) and trifluoromethyl methionine (TFM),<sup>7</sup> oxomethionine (OxM),<sup>7</sup> selenomethionine (SeM),<sup>7,8</sup> norleucine (Nle)<sup>7,8</sup>, and homocysteine (Hcy)<sup>9</sup> (Fig. 1B). These isostructural replacements resulted in minimal structural perturbation, as demonstrated by electronic absorption (UV-vis), electron paramagnetic resonance (EPR), and x-ray absorption spectra (XAS). We found a strong linear correlation between the hydrophobicity of the axial ligand (measured by the partition coefficient between octanol and water of the side chain, logP) and  $E^{\circ'}$  in Az (Fig. 1C), providing conclusive evidence that axial ligand hydrophobicity is a major determining factor of  $E^{\circ'}$ . Furthermore, we found this correlation to apply not only to Az but to all T1Cu centers.<sup>7</sup> The insight gained from these studies was subsequently used to tune  $E^{\circ'}$  in Az beyond the natural range of mononuclear T1Cu proteins<sup>10</sup> to eventually span the entire physiological  $E^{\circ'}$  range (*vide infra*),<sup>11</sup> a feature that had not been found in any single class of metalloprotein.

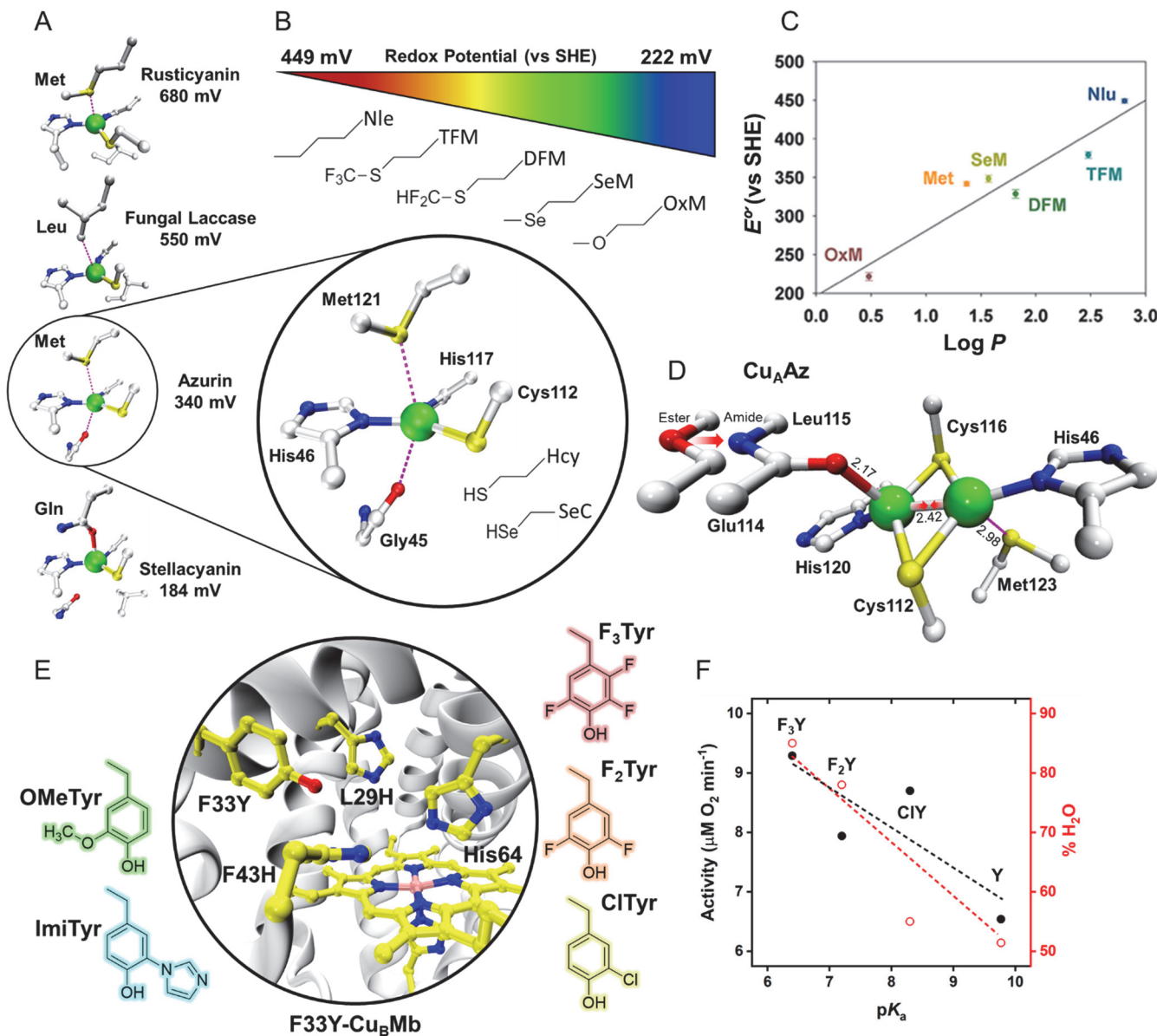


Figure 1. (A) Copper binding sites of T1Cu proteins and their  $E^{\circ}$  values, (B) Isostructural UAAs in Az and their  $E^{\circ}$  range. (C) Plot of  $E^{\circ}$  vs  $\log P$  in Az. Reproduced with permission from ref (7). Copyright 2006 American Chemical Society. (D) Crystal structure of Cu<sub>A</sub>-Az and the impact of a backbone ester substitution on Cu-Cu bond distance. (E) Crystal structure of F33Y-Cu<sub>B</sub>-Mb and UAA Tyr analogues. (F) Plot of O<sub>2</sub> reduction activity and proportion of H<sub>2</sub>O production vs  $\text{p}K_a$  (Data from ref (26)).

In addition to the axial ligand, we have replaced the conserved Cys112 in Az with selenocysteine (Sec) and Hcy (Fig. 1B). All T1Cu centers have low reorganization energy of the Cu(II)/Cu(I) redox transition due to an entatic state between the preferred geometries of Cu(I) and Cu(II) (also called the “rack” effect). The effect manifests as minimal changes in Cu-ligand bond lengths and bond angles during redox cycling. Replacing Cys112 by isostructural Sec resulted in a Cu(II)-Se bond that lengthened over the native Cu(II)-S bond only by the increase in covalent radius of Se over S (determined by XAS).<sup>12,13</sup> We found that Sec and Cys exhibit a similar degree of covalency with Cu due to the similar electronegativities of S and Se in the thiolate/selenolate ligand fragment.<sup>14</sup> Interestingly, the Cu-Se bond length varied by  $< 0.01$  Å during Cu(II)/Cu(I) redox transitions,<sup>13</sup> which is even less than the Cu(II)-S bond variation ( $\sim 0.08$  Å), suggesting that the larger Se atom is superior to S for enforcing the

entatic state. Based on these results, replacing Cys112 with Hcy (longer than Cys by one methyl group) was predicted to decrease the Cu(II)-S distance and increase Cu-S covalency. However, the Cu(II)-SHcy distance was longer than Cu(II)-SCys and displayed larger EPR parallel hyperfine splitting than in WT-Az while the Cu(II)-to-axial-Met interaction was shorter and stronger.<sup>15</sup> Hcy substitution, therefore, actually weakened Cu(II)-S covalency, probably due to a distortion of the Cu ion out of the entatic trigonal plane. The  $E^\circ'$  of Hcy112-Az was also found to be lower than WT-Az by 35 mV. These results suggest that the native Cu-SCys interaction is already nearly optimal and can only be surpassed by an isostructural Cu-Se substitution.

Heme-copper oxidase (HCO) and nitrous oxide reductase (N<sub>2</sub>OR) contain ET subunits with binuclear Cu centers (Cu<sub>A</sub>), and UAAs have been introduced to Cu<sub>A</sub> centers to fine-tune their functions. The Cu<sub>A</sub> center comprises two Cu ions, each bound by one His ligand and bridged by two Cys to form a diamond core motif (Fig. 1D)<sup>16,17</sup>. Each Cu ion is also coordinated by a weak axial ligand, i.e., Met on one Cu ion and a carbonyl of the peptide backbone on the other. Studies that have mutated the axial Met have found that, like T1Cu proteins, the axial Met tunes Cu<sub>A</sub>  $E^\circ'$  without increasing the inner-sphere reorganization energy. Indeed, the reorganization energy of Cu<sub>A</sub> is even lower than T1Cu, allowing Cu<sub>A</sub> to function with a smaller driving force.<sup>18-20</sup> An interesting and more challenging task is to tune the  $E^\circ'$  through the backbone carbonyl because it is not amenable to standard mutagenesis methods. We replaced the peptide bond between Glu114 and Leu115 with an ester linkage (Fig. 1D),<sup>21</sup> and the resulting depsipeptide created an axial carbonyl donor less basic than the native ligand. The metal center exhibited blue-shifted near-IR absorption of the Cu-Cu  $\psi \rightarrow \psi^*$  transition, evidence of a shorter Cu-Cu bond.<sup>21</sup> Interestingly, this change had minimal impact on  $E^\circ'$ , suggesting that, unlike T1Cu, the core structure of Cu<sub>A</sub> is resistant to variations in axial interactions.

HCO also contains a heme-Cu center that catalyzes reduction of O<sub>2</sub> to water. The heme is coordinated by a proximal His, and the nonheme Cu center (called Cu<sub>B</sub>) is bound by three His residues, one of which is cross-linked to a conserved Tyr. It has been hypothesized that the pK<sub>a</sub> and  $E^\circ'$  of the Tyr/Tyr-radical of the cross-linked AAs are important for proton and electron transfer;<sup>22</sup> however, because the Tyr-His cross-link is a product of post-translational modification, it cannot be directly probed via mutagenesis. We overcame this limitation with our previously reported structural and functional ArM model of HCO in sperm whale myoglobin (Mb) that contains a similar Cu<sub>B</sub> center (L29H/F43H-Mb), called Cu<sub>B</sub>Mb (Fig. 1E).<sup>23</sup> We found that simply introducing Tyr through either F33Y or G65Y mutation dramatically enhanced enzymatic activity, resulting in >1000 turnovers and high selectivity for complete 4e<sup>-</sup> reduction of O<sub>2</sub> to H<sub>2</sub>O over reactive oxygen species (ROS: superoxide, peroxide, and hydroxyl radical).<sup>24</sup> When combined with protein-protein interface design to improve ET from the native Mb redox partner, cytochrome *b*<sub>5</sub>, G65Y-Cu<sub>B</sub>Mb displayed activity similar to a native HCO.<sup>25</sup>

To probe the His/Tyr cross-link, we introduced UAA analogs of Tyr (Fig. 1E), such as 3-chlorotyrosine (CITyr), 3,5-difluorotyrosine (F<sub>2</sub>Tyr), and 2,3,5-trifluorotyrosine (F<sub>3</sub>Tyr), that progressively lower the pK<sub>a</sub> of the phenol ring from 10.0 (Tyr) to 6.4 (F<sub>3</sub>Tyr). We found that enzyme activity increased as the pK<sub>a</sub> decreased, as did the proportion of H<sub>2</sub>O production (Fig. 1F).<sup>26</sup> With the Tyr analog 3-methoxytyrosine (OMeY) we probed the role of phenolate E $^\circ'$  (179 mV lower than Tyr) without altering pK<sub>a</sub>. F33OMeY-Cu<sub>B</sub>Mb displayed significantly greater O<sub>2</sub> reduction activity and produced greater than 80% H<sub>2</sub>O (versus 51% in F33Y-Cu<sub>B</sub>Mb).<sup>27</sup> The correlated effects of lower E $^\circ'$  and pK<sub>a</sub> with UAA Tyr analogues were both direct observations of the role of Tyr as an active participant in oxidase activity through proton coupled ET. We then synthesized (S)-2-amino-3-(4-hydroxy-3-(1*H*-imidazol-1-yl)phenyl)propanoic acid (imiTyr) and incorporated it into Cu<sub>B</sub>Mb to create an *ortho*-imidazole-phenol linkage similar to native HCO.<sup>28</sup> The mutant imiTyrCu<sub>B</sub>Mb reconstituted with Cu(II) generated no more than 6% ROS, far superior to F33Y-Cu<sub>B</sub>Mb and capable of at least as many turnovers. A similar enhancement was found for ethyl diazoacetate mediated styrene cyclopropanation by Mb in the absence of reductant when we replaced the axial His93 with N<sub>δ</sub>-methylhistidine (NMH). NMH-Mb allowed us to capture an elusive carbennoid intermediate implicated in the P450 catalyzed reaction.<sup>29</sup> A final probe into the role of Tyr in HCO examined whether Tyr participates in ET via a tyrosyl radical that has been observed in HCO in the presence of H<sub>2</sub>O<sub>2</sub> but which had not been found definitively under native turnover conditions. We have observed a Tyr radical in F33Y-Cu<sub>B</sub>Mb by EPR spectroscopy both in the presence of O<sub>2</sub> under turnover conditions and by treatment with H<sub>2</sub>O<sub>2</sub>,<sup>30</sup> but it was unclear where the radical was localized. A definitive assignment of the engineered Tyr as the site of a tyrosyl radical was made possible by the unique EPR hyperfine splitting pattern provided by halogenated UAA Tyr analogues, directly implicating the Tyr radical as a mechanistic component in oxygen reduction.<sup>26</sup>

### 3. Understanding and Modulating Biological Function with Non-Native Metallocofactors

In addition to amino acids, proteins employ a diverse range of metal-containing cofactors to enhance their biological functions: a prominent example is the variety of heme cofactors found in HCOs. HCOs from different organisms contain hemes with different structures, such as heme *a*, *b*, *o*, and *d*, and have a wide range of  $E^\circ'$ .

Since all HCOs perform the same reaction with different driving forces, their heme variation raised the question of whether simply substituting one heme for another would modulate HCO activity. This question could be answered directly in HCO by extracting the native heme and replacing it with another variant. There are many examples of heme substitution leading to novel or modified activity, such as stereoselective and chemoselective cyclopropanation of olefins<sup>31,32</sup> and modified regioselectivity of fatty acid hydroxylation.<sup>33</sup> Because HCO is a membrane-bound protein with heme-dependent assembly, it has been difficult to extract and replace its native hemes while retaining function. We sought to address this question in Cu<sub>B</sub>Mb by replacing heme *b* with hemes containing monoformyl (MF) and diformyl (DF) substitutions (Fig. 2A-B) to mimic the formyl group in heme *a*. We found that heme E°' increased with increasing electron-withdrawing ability of the substitutions in the order of native heme *b*, MF-heme, and DF-heme (Fig. 2C).<sup>34</sup> In addition, the rate of O<sub>2</sub> reduction and enzyme turnover number were both positively correlated with heme E°' while ROS production remained essentially constant. Rapid stopped-flow kinetics studies found that increased heme E°' was associated with increases in the rates of ET, O<sub>2</sub> binding, O<sub>2</sub> dissociation, and a slight decrease in O<sub>2</sub> affinity.<sup>35</sup> DFT calculations of the active site with bound O<sub>2</sub> found heme E°' modulation significantly impacted the electronic charge of both Fe and O<sub>2</sub>, resulting in faster O<sub>2</sub> dissociation and reduced O<sub>2</sub> affinity at higher E°' values.

Nitric oxide reductase (NOR) is structurally homologous to HCO, but instead of a heme-Cu center that reduces O<sub>2</sub> (O-O bond cleavage), NOR utilizes a heme/nonheme Fe center to perform the two-electron reduction of NO to N<sub>2</sub>O (N-N bond formation). How the two enzymes are fine-tuned to perform their respective functions remains an area of active research. Despite similar active sites, the active heme in NORs exhibits much lower E°' (-178 mV to -59 mV) than HCOs (-39 mV to +480 mV). We tested whether E°' differentiates HCO vs. NOR activity by replacing the native heme *b* in a Mb-based NOR model (called Fe<sub>B</sub>Mb,<sup>36</sup> Fig. 2D) with non-native MF-heme and DF-heme cofactors to generate a set of NOR ArMs with heme E°' systematically varied from -130 mV to +148 mV. Decreasing E°' resulted in large enhancements in NO association and heme-nitrosyl decay rates (Fig. 2E). These results indicate that NORs control E°' to maximize their enzymatic efficiency and achieve a balance between two antagonistic processes: fast NO binding and decay of dinitrosyl species are facilitated by low E°', while fast ET is facilitated by high E°'. Only when E°' is optimally tuned in Fe<sub>B</sub>Mb (MF-heme) does the protein achieve multiple (>35) turnovers of N-N bond formation, a feat that had not been previously achieved in any model catalyst. These results also addressed a long-standing question in bioenergetics of selective cross-reactivity between HCO and NOR: only HCOs with low heme E°' in a similar range to NORs (between -59 mV and +200 mV) exhibit NOR reactivity. Our studies using non-native metallocofactors, therefore, not only resolved several issues that were difficult to address by studying native enzymes, but also demonstrated the extent to which they modulate substrate affinity, ET rate, and enzymatic activity.

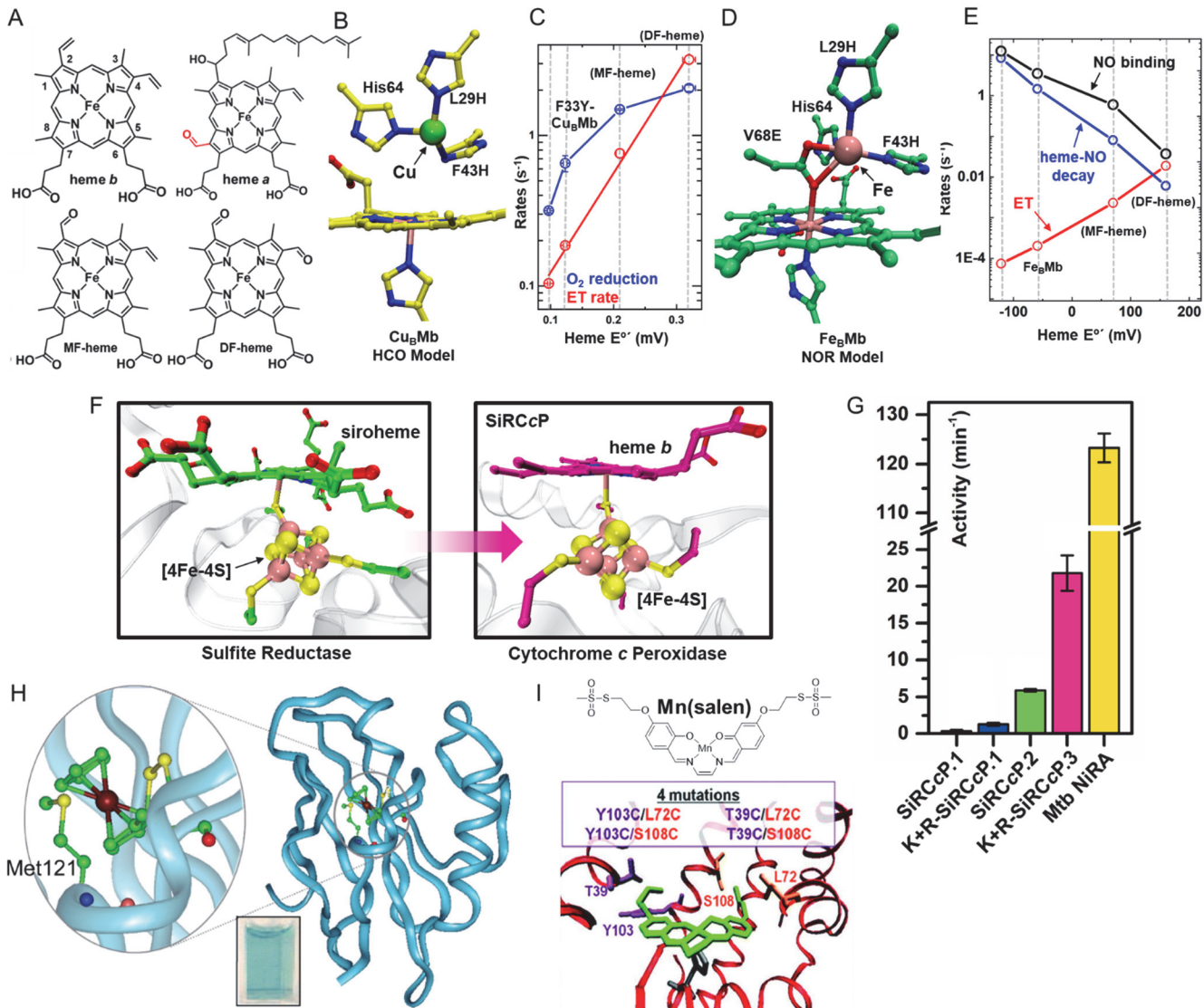


Figure 2. (A) Various heme cofactors. (B) Crystal structure of the ArM model of HCO in Mb (Cu<sub>B</sub>Mb) and (C) Rates of O<sub>2</sub> reduction and ET vs heme  $E^{\circ'}$  in Cu<sub>B</sub>Mb (data from ref (34)). (D) Crystal structure of the ArM model of NOR in Mb (Fe<sub>B</sub>Mb). (E) Rates of ET, NO binding, and heme-NO decay vs heme  $E^{\circ'}$  in Fe<sub>B</sub>Mb (data from ref (36)). (F) Crystal structure of heme-[4Fe-4S] cofactor from SiR and corresponding computational model in CcP (SiRCCP). (G) SiR activity, measured by the rates of SO<sub>3</sub><sup>2-</sup> reduction in SiRCCP containing SCS mutations to improve SO<sub>3</sub><sup>2-</sup> binding with Lys/Arg and tuning of [4Fe-4S], in comparison with that of a native SiR. Reproduced with permission from ref (40). Copyright 2018 American Association for the Advancement of Sciences. (H) Computational model of ferrocene (Fc) in Az replacing the native Cu ion and the resulting blue bio-organometallic complex in solution. Reproduced with permission from ref (41). Copyright 2005 American Chemical Society. (I) Computational model of Mn(salen) in the Mb replacing the native heme cofactor. Reproduced with permission from ref (44). Copyright 2011 American Chemical Society.

Non-native metallocofactors have also played an important role in decoding reaction mechanisms. Despite decades of research on NOR, the mechanism for N-N coupling remained unresolved. Three reaction pathways have been proposed: the *trans* pathway proceeds through one NO binding each to the heme Fe and nonheme Fe (called Fe<sub>B</sub>); the *cis* pathway proceeds through radical coupling of NO to heme-bound NO; and the *cis*-Fe<sub>B</sub> pathway proceeds by both NO binding to the nonheme Fe. By replacing heme *b* in Fe<sub>B</sub>Mb with isostructural Zn-protoporphyrin-IX, we could obtain isolate spectroscopic information of the non-heme Fe to investigate the

electronic and functional properties of the nonheme  $\text{Fe}_\text{B}$  nitrosyl complex.<sup>38,39</sup> The electronic state of the  $\{\text{FeNO}\}^7$  complex was best described as high spin ferrous Fe ( $S = 2$ ) antiferromagnetically coupled to a NO radical ( $S = 1/2$ )  $[\text{Fe}^{2+}\text{-NO}^\bullet]$ , consistent with the radical coupling process of the *trans* mechanism of NO reduction.

A subtle (yet important) take-away from early-stage ArM models is that although native enzymes exhibit their highest activities with specific cofactors, such as heme *a*, ArMs can exhibit some degree of native activity with simpler cofactors, such as heme *b*. Much of the difference in activity between a homogenous metal catalyst and a metalloenzyme may derive from stabilizing interactions with the protein matrix and the bound metal catalyst. Recently, we have reported an ArM in cytochrome *c* peroxidase (called SiRCcP, Fig. 2F) of the heme-[4Fe-4S] active site of sulfite reductase (SiR) by creating a [4Fe-4S]-binding site adjacent to the native heme *b* cofactor.<sup>37</sup> SiRCcP was made to exhibit up to ~20% the activity of a native SiR by incorporation of substrate binding residues and SCS interactions to the [4Fe-4S], a feat that had not been achieved by small-molecule models. Furthermore, SiRCcP was capable of converting sulfite to hydrogen sulfide (Fig. 2G), a  $6\text{e}^-$  process, in a proportion similar to native dissimilatory SiR using Fe-protoporphyrin-IX instead of the SiR Fe-sirohydrochlorin cofactor. This success with SiRCcP, as a complement to the studies with  $\text{Cu}_\text{B}\text{Mb}$  and  $\text{Fe}_\text{B}\text{Mb}$ , demonstrates that, while the structure of the metallocofactor can exert strong control over reactivity, much of the vast differences in turnover rate and stability between naturally evolved enzymes and artificial catalysts derives from the protein matrix.

In addition to replacing one biological cofactor with another, we have also incorporated abiological cofactors into metalloproteins to impart new function. Most organometallic complexes are not soluble or stable in water. Ferrocene (Fc) is barely soluble in water, and its oxidized product (ferrocenium) decomposes in water, especially at high pH. We were able to stabilize Fc in Az, even at high pH, by selective attachment of 2-[(methylsulfonyl)thio]ethylferrocene to the conserved residue Cys112 in the native Cu binding site (Fig. 2H) and were able to modulate its  $E^\circ'$  by SCS mutation.<sup>40</sup> We have also investigated how attachment of non-native metallocofactors to the protein scaffold affects their enantioselectivity and chemoselectivity. Previous studies have incorporated metal complexes such as Cr(salophen) into the Mb heme site. However, the enantioselectivity of thioanisole sulfoxidation was low.<sup>41</sup> To limit the conformational flexibility of the non-native ligand, we covalently attached methane thiosulfonate functionalized Mn(salen) to Mb by either one or two mutant Cys residues (Fig. 2I). Two covalent attachments resulted in a 5-fold rate enhancement over a single covalent attachment and increased enantioselective excess (S) to 51% (versus 12%).<sup>42</sup> Attachment to the protein scaffold prevents dimerization of the Mn(salen) complex and restricts water access to the active metal, and changing the dual anchoring positions modulated ee (S) by ~80%,<sup>43</sup> demonstrating that even small orientation changes in a protein scaffold can substantially modify the function of a conjugated metal catalyst. The protein scaffold can also create a “solvent cage” effect for catalysis: embedding Mn(salen) within the Mb scaffold prevents formation of the overoxidized sulfone product.<sup>44</sup> Comparison to free Mn(salen) in non-polar and proton-donating solvents revealed that protonation heavily favored sulfoxide formation. The Mb scaffold also tuned substrate access: an A71S mutation to increase polarity in the substrate-access channel allows the polar sulfoxide product to re-enter the active site, altering chemoselectivity of the enzyme for sulfone production. More recently, Mn-porphycene substituted Mb has been shown to activate inert C-H bonds for ethylbenzene hydroxylation via high-valent Mn(V)-oxo species similar to the cytochrome P450.<sup>45</sup>

#### 4. Understanding and Modulating Biological Function with Non-Native Metal Ions

Natural enzymes can bind only a limited number of metal ions, and most metalloproteins lose stability or function when their native metals are removed or replaced. Substituting native metal ions for others could help us understand how functional metals are selected, how their functions are controlled, and how to potentially confer new functions. For example, the Cu in T1Cu proteins has been replaced with Co(II) and Zn(II) to probe ET function.<sup>1-3</sup> To confer new biological functions, the Holland group has shown that metal-free WT-Az can bind Fe(II) weakly, but Fe(II)-Az was not redox active.<sup>46</sup> Shafaat and coworkers proposed that the Cu environment of Az, whose high  $E^\circ'$  is evidence of its preference for Cu(I) over Cu(II), discouraged oxidation to Fe(III). Replacement of the axial Met by Ala creates a reactive binding site for ligands such as cyanide and azide, but it does not change the PCS or electronic structure of bound Fe(II).<sup>46</sup> We were able to achieve a redox-active Fe(II)/Fe(III) couple with similar  $E^\circ'$  to WT-Az (+327 mV) by mutation of the axial Met to a Glu (M121E-Az, Fig. 3A) to stabilize the Fe(III) oxidation state. This redox-active mutant exhibited superoxide reductase (SOR) activity, transforming an ET protein into an enzyme for the first time.<sup>47</sup> To increase the SOR activity of M121E-Az, we looked for residues in the SCS of SOR and found a Lys that is ~8 Å distal to the Cys ligand, which has been implicated in recruiting superoxide to the mononuclear iron active site. Introducing this distal Lys residue into Az by M44K mutation increased the SOR activity by two orders of magnitude. Therefore, by non-native metal substitution and further tuning of the SCS, it was possible to create a non-heme Fe-based ArM in Az from a Cu-based ET protein.

Ni(II) can also effectively replace Cu in Az. While the Cu(II)/Cu(I) redox couple in Az has been tuned over a range of 900 mV (from +90 mV to +970 mV) by SCS mutations, replacing Cu(II) with Ni(II) shifts  $E^\circ$  by nearly -1 V, creating a set of mutant variants in a single ET protein that span the entire 2 V physiological redox range (-954 to +970 mV, Fig. 3B-F).<sup>11</sup> These Ni- and Cu-Az based ArMs may find a wide range of applications as redox agents for biochemical and biophysical studies. Recently, Shafaat and coworkers also found that Ni-substituted Az creates a protein with a stable Ni(II/I) redox couple that lowers  $E^\circ$  by ~900 mV to -590 mV (vs. +310 mV in Cu-Az) while preserving a trigonal planar metal binding geometry.<sup>48</sup> With a mutation of the axial Met to Ala to create a small-molecule binding site, Ni-M121A-Az was found to quantitatively bind CO and reversibly bind a methyl group in the presence of CH<sub>3</sub>, making it possible to use Ni-Az as a model for CO-dehydrogenase/acetyl CoA-synthase (Fig. 3A).<sup>49</sup> Further, substituting Ni for the native Fe of rubredoxin created an active H<sub>2</sub> evolution ArM that is oxygen tolerant and displays electrochemical activity approaching native [NiFe] hydrogenase with low overpotential.<sup>50</sup> Photocatalytic activity could be achieved and modulated by selective conjugation of a Ru(bpy)<sub>3</sub> complex,<sup>51</sup> and detailed spectroscopic and computational characterization of the model elucidated a thiol-inversion mechanism of Ni(III)-hydride formation that is directly applicable to native [NiFe] hydrogenase.<sup>52,53</sup>

In addition to mononuclear metalloproteins, heteronuclear bimetallic enzymes have also benefited from replacing the native with non-native metal ions. Despite highly homologous active sites, why a nonheme Cu atom was selected for O<sub>2</sub> reduction in HCO but nonheme Fe was selected for NO reduction in NOR had never been directly probed because removing the nonheme metal ion of either enzyme destabilizes it.<sup>54</sup> Our ArMs (Cu<sub>B</sub>Mb and Fe<sub>B</sub>Mb), however, were sufficiently small and malleable to allow facile metal substitution. When we replaced the nonheme Fe(II) in Fe<sub>B</sub>Mb with Cu(I), O<sub>2</sub> reduction activity increased 3-fold.<sup>55</sup> A further study to explain this effect found that the identity of the nonheme metal had minimal impact on heme  $E^\circ$ , but  $E^\circ$  of Cu(II)/Cu(I) is +128 mV higher than nonheme Fe(II)/Fe(III). Since the rate of O<sub>2</sub> reduction is limited by ET, a stronger driving force for ET to bound O<sub>2</sub> is partially responsible for the observed rate enhancement with Cu. In addition, examination of the O-O bond length by resonance Raman spectroscopy and subsequent DFT calculations found that the O-O bond was weaker with nonheme Cu than nonheme Fe. We attribute this effect to the *d*-electron configuration of Cu (*d*<sup>9</sup>) that allows it to donate more electron density to O<sub>2</sub> than Fe (*d*<sup>5</sup>), weakening the O-O bond to facilitate O<sub>2</sub> cleavage more effectively (Fig. 3G).

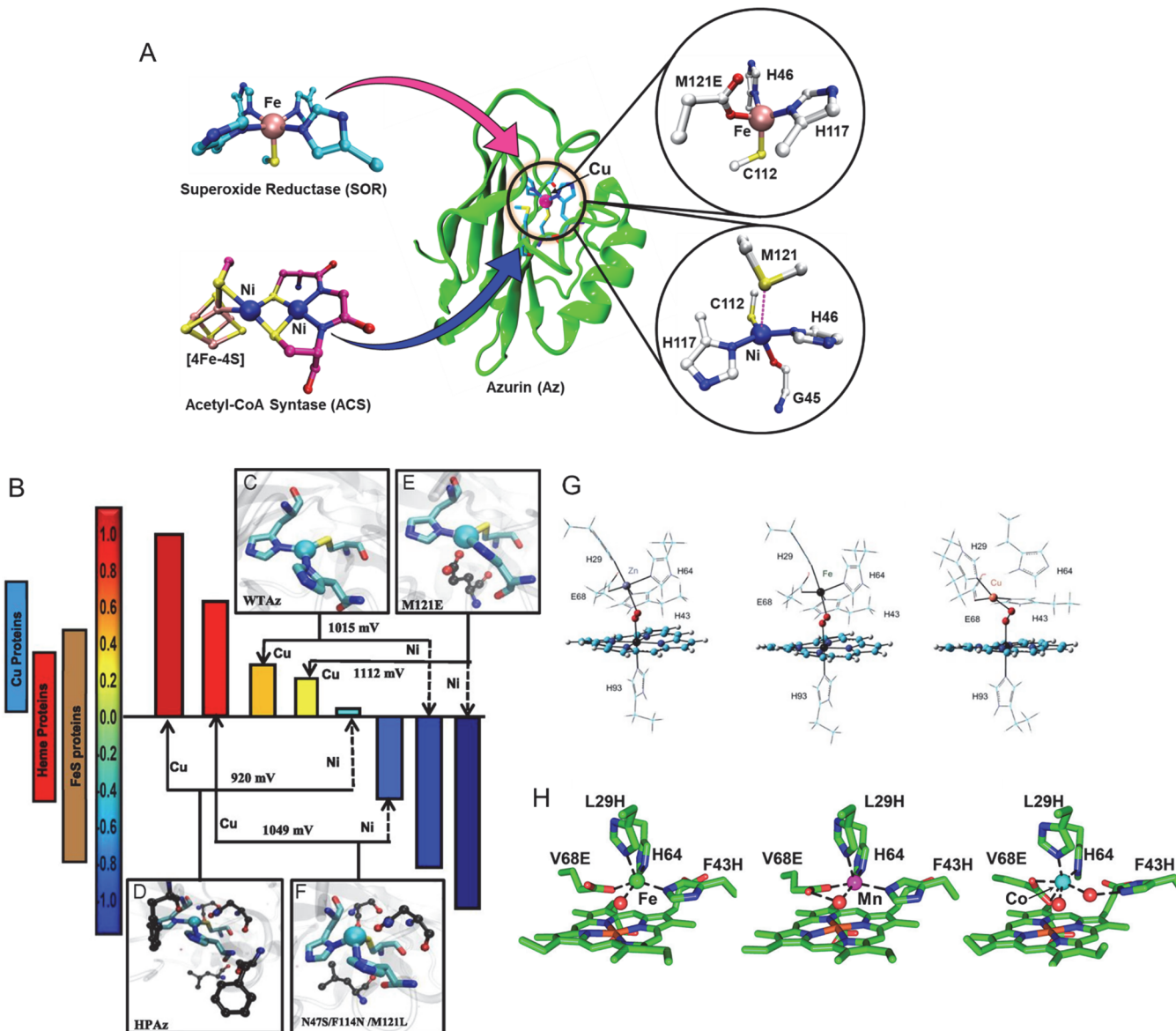


Figure 3. (A) Crystal structures of metal-binding sites in SOR and ACS and their models in Az; (B) The entire physiological  $E^{\circ'}$  range achieved in Az by five mutants and two metal ions; (C-F) Crystal structures of native and mutant Az with their respective Cu-bound and Ni-bound Cu(I/II) or Ni(I/II) redox potentials. Reproduced with permission from ref. 11. Copyright 2015 National Academy of Sciences; (G) DFT-optimized structures of  $O_2$ -bound Cu<sub>B</sub>Mb with Zn(II), Fe(II), or Cu(II) in the nonheme metal site. Reproduced with permission from ref. 55. Copyright 2017 Springer Nature; (H) Crystal structures of Fe<sub>B</sub>Mb with Fe(II), Mn(II), and Co(II) in the nonheme metal site. Reproduced with permission from ref. 56. Copyright 2017 American Chemical Society.

The observation that nonheme Zn ( $d^{10}$ ) still weakened the O-O bond relative to Fe<sub>B</sub>Mb without a nonheme metal raised the question of whether other nonheme metal ions could facilitate O<sub>2</sub> reduction. When the nonheme metal in Fe<sub>B</sub>Mb was replaced with Mn(II) or Co(II),<sup>56</sup> both proteins displayed oxygen reduction rates similar to Fe-Fe<sub>B</sub>Mb, but the proportion of ROS decreased as Mn > Fe > Co (from 7% to 1%), which matched a trend of increasing total turnover number (5.1 > 13.4 > 82.5). Unlike Fe and Cu, redox transitions were not observed in Mn or Co during catalysis. Stopped-flow UV-vis and vibrational spectroscopy of the O-O and M-O bonds revealed that, while both Mn and Co induce similar O-O bond lengthening, the Co-O distance is 0.274 Å shorter than the Mn-O distance, and the rate of heme-oxy intermediate formation and decay (not observed with redox-active Fe and Cu nonheme metals) was much slower with nonheme Co than with Mn or Zn. Fe<sub>B</sub>Mb co-crystallized with each of the three metals revealed

highly similar binding geometries for Mn(II) and Fe(II), but the Co(II) assumed an octahedral geometry with bidentate coordination by E68 which may also stabilize the heme-oxy intermediate (Fig. 3H). Taken together, replacing the nonheme metal in Fe<sub>B</sub>Mb with metals that have different *d*-electron configurations revealed that, while redox activity plays an important role in O<sub>2</sub> reduction, the geometry and Lewis acidity of even a redox-inactive metal is important for determining turnover rate. We tested NO reduction activity with the same nonheme metals (Fe, Co, and Zn)<sup>57</sup> and found that Fe<sub>B</sub>Mb could achieve multiple turnovers regardless of the nonheme metal. Thus, NOR activity with redox-inactive Zn(II) further supports the viability of a one-electron semi-reduced pathway for the reduction of NO. Overall, by adding non-native metal ions to enzymes, we have deconvoluted reaction mechanisms that may be useful for designing next-generation catalysts.

## 5. Conclusion and Outlook

ArMs promise enormous potential to perform abiological reactions for many chemical, biotechnological, and pharmaceutical applications. The missing key to unlock their potential is a fundamental understanding of how a single and (in many cases) simple PCS performs many functional roles. If we can understand this, it should be possible to design ArMs at least as active as native enzymes. We have summarized several avenues to this goal through UAAs, and non-native metal ions and metallocofactors that probe and modulate metalloprotein function. With these tools we have made ArMs with activity that matches, and—in a few cases—surpasses native enzymes, and we have shown that non-covalent interactions, such as hydrogen bonding and hydrophobicity, in the SCS are very important for tuning redox, electronic, and other functional properties. In many cases, fine-tuning E<sup>o</sup> alone has proven to be critical both for ET function and for catalysis, such as HCO/NOR activity. Moreover, the protein matrix is critical for tuning the reactivity, stability, and turnover rates of organometallic cofactors. A key revelation from our efforts is the identification of common principles that govern the effects of SCS interactions and behave predictably for metal centers across different proteins. Systematic modulation of these interactions (e.g. hydrophobicity) is likely to yield the desired effects in most systems. These observations are valuable to all ArM systems: while it was once sufficient to demonstrate that ArMs can minimally catalyze abiological reactions, future ArMs must demonstrate deliberate control over activity.

While progress has certainly been made in this area, we have identified only a small fraction of the interactions that can be generally transferred to ArMs to fine-tune their functions. Quantitative probing of a given SCS interactions in different metal binding sites has revealed that the magnitude of any one interaction varies greatly from one metalloprotein to another, suggesting that there must be many factors controlling their functional properties that we either cannot yet fully account for or have yet to recognize. Because the SCS interactions are predominantly subtle and heavily interconnected, it has been difficult to characterize the effects of these interactions with precision. Most of these interactions have minimal effects on functional properties while a few others have huge effects. Furthermore, most SCS interactions exert their effects dynamically and in the transition state. Thus, we lack necessary information to predict these effects for most proteins. To address these issues, it is vital to develop spectroscopic and—especially—robust computational techniques able to detect and quantify weak interactions in catalytic intermediates with precision to develop a more complete profile of protein metal-ligand interactions. Bioinformatic analysis of metalloprotein structural databases to identify conserved SCS features and determine which features are correlated with certain functions will also be helpful. Finally, while UAAs and non-native metallocofactors have proven to be powerful tools, they remain difficult to synthesize and incorporate into ArMs. Methods to improve synthesis yields and incorporation efficiency will improve their utility for both fundamental studies and practical applications.

## Corresponding Author

\*Email: yi-lu@illinois.edu

## ORCID

0000-0003-1221-6709

## Notes

The authors declare no competing financial interest

## Biographical Information

**Evan N. Mirts** is a post-doctoral researcher at the University of Illinois at Urbana-Champaign. He received his B.S. in Biology from Truman State University (2012) and his Ph.D. in Biophysics and Computational Biology from the University of Illinois at Urbana-Champaign (2018). His research interests are the development of design processes for non-native metalloenzymes with complex metal cofactors.

**Ambika Bhagi-Damodaran** is an Assistant Professor of Chemistry at the University of Minnesota, Twin Cities. Ambika completed her Ph.D. at the University of Illinois, Urbana-Champaign in 2016 and postdoctoral research at University of California, San Francisco. Her current research investigates metalloenzyme-based redox signaling pathways as potential therapeutic targets for cancer and infectious diseases.

**Yi Lu** is a Jay and Ann Schenck Professor in the Department of Chemistry at the University of Illinois at Urbana-Champaign. He received his B.S. degree from Peking University in 1986 and his Ph.D. degree from UCLA in 1992 under Dr. Joan S. Valentine. After 2 years of postdoctoral research in Dr. Harry B. Gray's group at Caltech, he started his own independent career at UIUC in 1994. His group interests are in bioinorganic, biomaterial, and bioanalytical chemistry.

## Acknowledgments

The Lu group research described in this account has been supported by the US National Science Foundation (under award CHE 17-10241), National Institute of Health (under award GM06211) and Department of Energy's Center for Advanced Bioenergy and Bioproducts Innovation (Office of Science, Office of Biological and Environmental Research, under award DE-SC0018420).

## References

- (1) Lu, Y. Biosynthetic Inorganic Chemistry. *Angew. Chem. Int. Edit.* **2006**, *45* (34), 5588–5601. DOI: 10.1002/anie.200600168.
- (2) Lu, Y.; Yeung, N.; Sieracki, N.; Marshall, N. M. Design of Functional Metalloproteins. *Nature* **2009**, *460* (7257), 855–862. DOI: 10.1038/nature08304.
- (3) Yu, Y.; Hu, C.; Xia, L.; Wang, J. Artificial Metalloenzyme Design with Unnatural Amino Acids and Non-Native Cofactors. *ACS Catal.* **2018**, *8* (3), 1851–1863. DOI: 10.1021/acscatal.7b03754.
- (4) Warren, J. J.; Lancaster, K. M.; Richards, J. H.; Gray, H. B. Inner- and Outer-Sphere Metal Coordination in Blue Copper Proteins. *J. Inorg. Biochem.* **2012**, *115*, 119–126. DOI: 10.1016/j.jinorgbio.2012.05.002.
- (5) Liu, J.; Chakraborty, S.; Hosseinzadeh, P.; Yu, Y.; Tian, S.; Petrik, I.; Bhagi, A.; Lu, Y. Metalloproteins Containing Cytochrome, Iron–Sulfur, or Copper Redox Centers. *Chem. Rev.* **2014**, *114* (8), 4366–4469. DOI: 10.1021/cr400479b.
- (6) Clark, K. M.; van der Donk, W. A.; Lu, Y. Chapter 5 Expressed Protein Ligation for Metalloprotein Design and Engineering. In *Methods in Enzymology*; Muir, T. W., Abelson, J. N., Eds.; Non-Natural Amino Acids; Academic Press, 2009; Vol. 462, pp 97–115. DOI: 10.1016/S0076-6879(09)62005-X.
- (7) Garner, D. K.; Vaughan, M. D.; Hwang, H. J.; Savelieff, M. G.; Berry, S. M.; Honek, J. F.; Lu, Y. Reduction Potential Tuning of the Blue Copper Center in *Pseudomonas aeruginosa* Azurin by the Axial Methionine as Probed by Unnatural Amino Acids. *J. Am. Chem. Soc.* **2006**, *128* (49), 15608–15617. DOI: 10.1021/ja062732i.
- (8) Berry, S. M.; Ralle, M.; Low, D. W.; Blackburn, N. J.; Lu, Y. Probing the Role of Axial Methionine in the Blue Copper Center of Azurin with Unnatural Amino Acids. *J. Am. Chem. Soc.* **2003**, *125* (29), 8760–8768. DOI: 10.1021/ja029699u.

(9) Clark, K. M.; Yu, Y.; Marshall, N. M.; Sieracki, N. A.; Nilges, M. J.; Blackburn, N. J.; van der Donk, W. A.; Lu, Y. Transforming a Blue Copper into a Red Copper Protein: Engineering Cysteine and Homocysteine into the Axial Position of Azurin Using Site-Directed Mutagenesis and Expressed Protein Ligation. *J. Am. Chem. Soc.* **2010**, *132* (29), 10093–10101. DOI: 10.1021/ja102632p.

(10) Marshall, N. M.; Garner, D. K.; Wilson, T. D.; Gao, Y.-G.; Robinson, H.; Nilges, M. J.; Lu, Y. Rationally Tuning the Reduction Potential of a Single Cupredoxin beyond the Natural Range. *Nature* **2009**, *462* (7269), 113–116. DOI: 10.1038/nature08551.

(11) Hosseinzadeh, P.; Marshall, N. M.; Chacón, K. N.; Yu, Y.; Nilges, M. J.; New, S. Y.; Tashkov, S. A.; Blackburn, N. J.; Lu, Y. Design of a Single Protein That Spans the Entire 2–V Range of Physiological Redox Potentials. *PNAS* **2016**, *113* (2), 262–267. DOI: 10.1073/pnas.1515897112.

(12) Berry, S. M.; Gieselman, M. D.; Nilges, M. J.; van der Donk, W. A.; Lu, Y. An Engineered Azurin Variant Containing a Selenocysteine Copper Ligand. *J. Am. Chem. Soc.* **2002**, *124* (10), 2084–2085. DOI: 10.1021/ja0169163.

(13) Ralle, M.; Berry, S. M.; Nilges, M. J.; Gieselman, M. D.; van der Donk, W. A.; Lu, Y.; Blackburn, N. J. The Selenocysteine-Substituted Blue Copper Center: Spectroscopic Investigations of Cys112SeCys Pseudomonas Aeruginosa Azurin. *J. Am. Chem. Soc.* **2004**, *126* (23), 7244–7256. DOI: 10.1021/ja031821h.

(14) Sarangi, R.; Gorelsky, S. I.; Basumallik, L.; Hwang, H. J.; Pratt, R. C.; Stack, T. D. P.; Lu, Y.; Hodgson, K. O.; Hedman, B.; Solomon, E. I. Spectroscopic and Density Functional Theory Studies of the Blue–Copper Site in M121SeM and C112SeC Azurin: Cu–Se Versus Cu–S Bonding. *J. Am. Chem. Soc.* **2008**, *130* (12), 3866–3877. DOI: 10.1021/ja076495a.

(15) M. Clark, K.; Yu, Y.; Donk, W. A. van der; J. Blackburn, N.; Lu, Y. Modulating the Copper–Sulfur Interaction in Type 1 Blue Copper Azurin by Replacing Cys112 with Nonproteinogenic Homocysteine. *Inorg. Chem. Front.* **2014**, *1* (2), 153–158. DOI: 10.1039/C3QI00096F.

(16) Kelly, M.; Lappalainen, P.; Talbo, G.; Haltia, T.; Oost, J. van der; Saraste, M. Two Cysteines, Two Histidines, and One Methionine Are Ligands of a Binuclear Purple Copper Center. *J. Biol. Chem.* **1993**, *268* (22), 16781–16787.

(17) Robinson, H.; Ang, M. C.; Gao, Y.-G.; Hay, M. T.; Lu, Y.; Wang, A. H.-J. Structural Basis of Electron Transfer Modulation in the Purple CuA Center. *Biochemistry* **1999**, *38* (18), 5677–5683. DOI: 10.1021/bi9901634.

(18) Hwang, H. J.; Berry, S. M.; Nilges, M. J.; Lu, Y. Axial Methionine Has Much Less Influence on Reduction Potentials in a CuA Center than in a Blue Copper Center. *J. Am. Chem. Soc.* **2005**, *127* (20), 7274–7275. DOI: 10.1021/ja0501114.

(19) Ledesma, G. N.; Murgida, D. H.; Ly, H. K.; Wackerbarth, H.; Ulstrup, J.; Costa-Filho, A. J.; Vila, A. J. The Met Axial Ligand Determines the Redox Potential in CuA Sites. *J. Am. Chem. Soc.* **2007**, *129* (39), 11884–11885. DOI: 10.1021/ja0731221.

(20) Tsai, M.-L.; Hadt, R. G.; Marshall, N. M.; Wilson, T. D.; Lu, Y.; Solomon, E. I. Axial Interactions in the Mixed-Valent Cu<sub>A</sub> Active Site and Role of the Axial Methionine in Electron Transfer. *PNAS* **2013**, *110* (36), 14658–14663. DOI: 10.1073/pnas.1314242110.

(21) M. Clark, K.; Tian, S.; Donk, W. A. van der; Lu, Y. Probing the Role of the Backbone Carbonyl Interaction with the Cu A Center in Azurin by Replacing the Peptide Bond with an Ester Linkage. *Chem. Commun.* **2017**, *53* (1), 224–227. DOI: 10.1039/C6CC07274G.

(22) Kaila, V. R. I.; Johansson, M. P.; Sundholm, D.; Laakkonen, L.; Wikström, M. The Chemistry of the CuB Site in Cytochrome c Oxidase and the Importance of Its Unique His–Tyr Bond. *Biochim. Biophys. Acta, Bioenerg.* **2009**, *1787* (4), 221–233. DOI: 10.1016/j.bbabiobio.2009.01.002.

(23) Sigman, J. A.; Kwok, B. C.; Lu, Y. From Myoglobin to Heme-Copper Oxidase: Design and Engineering of a CuB Center into Sperm Whale Myoglobin. *J. Am. Chem. Soc.* **2000**, *122* (34), 8192–8196.

(24) Miner, K. D.; Mukherjee, A.; Gao, Y.-G.; Null, E. L.; Petrik, I. D.; Zhao, X.; Yeung, N.; Robinson, H.; Lu, Y. A Designed Functional Metalloenzyme That Reduces O<sub>2</sub> to H<sub>2</sub>O with Over One Thousand Turnovers. *Angew. Chem. Int. Edit.* **2012**, *51* (23), 5589–5592. DOI: 10.1002/anie.201201981.

(25) Yu, Y.; Cui, C.; Liu, X.; Petrik, I. D.; Wang, J.; Lu, Y. A Designed Metalloenzyme Achieving the Catalytic Rate of a Native Enzyme. *J. Am. Chem. Soc.* **2015**, *137* (36), 11570–11573. DOI: 10.1021/jacs.5b07119.

(26) Yu, Y.; Lv, X.; Li, J.; Zhou, Q.; Cui, C.; Hosseinzadeh, P.; Mukherjee, A.; Nilges, M. J.; Wang, J.; Lu, Y. Defining the Role of Tyrosine and Rational Tuning of Oxidase Activity by Genetic Incorporation of Unnatural Tyrosine Analogs. *J. Am. Chem. Soc.* **2015**, *137* (14), 4594–4597. DOI: 10.1021/ja5109936.

(27) Yu, Y.; Zhou, Q.; Wang, L.; Liu, X.; Zhang, W.; Hu, M.; Dong, J.; Li, J.; Lv, X.; Ouyang, H.; Li, H.; Gao, F.; Gong, W.; Lu, Y. Significant Improvement of Oxidase Activity through the Genetic Incorporation of a Redox-Active Unnatural Amino Acid. *Chem. Sci.* **2015**, *6* (7), 3881–3885. DOI: 10.1039/C5SC01126D.

(28) Liu, X.; Yu, Y.; Hu, C.; Zhang, W.; Lu, Y.; Wang, J. Significant Increase of Oxidase Activity through the Genetic Incorporation of a Tyrosine–Histidine Cross-Link in a Myoglobin Model of Heme–Copper Oxidase. *Angew. Chem. Int. Edit.* **2012**, *51* (18), 4312–4316. DOI: 10.1002/anie.201108756.

(29) Hayashi, T.; Tinzl, M.; Mori, T.; Krengel, U.; Proppe, J.; Soetbeer, J.; Klose, D.; Jeschke, G.; Reiher, M.; Hilvert, D. Capture and Characterization of a Reactive Haem–Carbenoid Complex in an Artificial Metalloenzyme. *Nat. Catal.* **2018**, *1* (8), 578. DOI: 10.1038/s41929-018-0105-6.

(30) Yu, Y.; Mukherjee, A.; Nilges, M. J.; Hosseinzadeh, P.; Miner, K. D.; Lu, Y. Direct EPR Observation of a Tyrosyl Radical in a Functional Oxidase Model in Myoglobin during Both H<sub>2</sub>O<sub>2</sub> and O<sub>2</sub> Reactions. *J. Am. Chem. Soc.* **2014**, *136* (4), 1174–1177. DOI: 10.1021/ja4091885.

(31) Sreenilayam, G.; Moore, E. J.; Steck, V.; Fasan, R. Stereoselective Olefin Cyclopropanation under Aerobic Conditions with an Artificial Enzyme Incorporating an Iron-Chlorin E6 Cofactor. *ACS Catal.* **2017**, *7* (11), 7629–7633. DOI: 10.1021/acscatal.7b02583.

(32) Moore, E. J.; Steck, V.; Bajaj, P.; Fasan, R. Chemoselective Cyclopropanation over Carbene Y–H Insertion Catalyzed by an Engineered Carbene Transferase. *J. Org. Chem.* **2018**, *83* (14), 7480–7490. DOI: 10.1021/acs.joc.8b00946.

(33) Omura, K.; Aiba, Y.; Onoda, H.; Stanfield, J. K.; Ariyasu, S.; Sugimoto, H.; Shiro, Y.; Shoji, O.; Watanabe, Y. Reconstitution of Full-Length P450BM3 with an Artificial Metal Complex by Utilising the Transpeptidase Sortase A. *Chem. Commun.* **2018**, *54* (57), 7892–7895. DOI: 10.1039/C8CC02760A.

(34) Bhagi-Damodaran, A.; Petrik, I. D.; Marshall, N. M.; Robinson, H.; Lu, Y. Systematic Tuning of Heme Redox Potentials and Its Effects on O<sub>2</sub> Reduction Rates in a Designed Oxidase in Myoglobin. *J. Am. Chem. Soc.* **2014**, *136* (34), 11882–11885. DOI: 10.1021/ja5054863.

(35) Bhagi-Damodaran, A.; Kahle, M.; Shi, Y.; Zhang, Y.; Ädelroth, P.; Lu, Y. Insights Into How Heme Reduction Potentials Modulate Enzymatic Activities of a Myoglobin-Based Functional Oxidase. *Angew. Chem. Int. Ed.* **2017**, *56* (23), 6622–6626. DOI: 10.1002/anie.201701916.

(36) Lin, Y.-W.; Yeung, N.; Gao, Y.-G.; Miner, K. D.; Tian, S.; Robinson, H.; Lu, Y. Roles of Glutamates and Metal Ions in a Rationally Designed Nitric Oxide Reductase Based on Myoglobin. *PNAS* **2010**, *107* (19), 8581–8586. DOI: 10.1073/pnas.1000526107.

(37) Mirts, E. N.; Petrik, I. D.; Hosseinzadeh, P.; Nilges, M. J.; Lu, Y. A Designed Heme-[4Fe-4S] Metalloenzyme Catalyzes Sulfite Reduction like the Native Enzyme. *Science* **2018**, *361* (6407), 1098–1101. DOI: 10.1126/science.aat8474.

(38) Chakraborty, S.; Reed, J.; Ross, M.; Nilges, M. J.; Petrik, I. D.; Ghosh, S.; Hammes-Schiffer, S.; Sage, J. T.; Zhang, Y.; Schulz, C. E.; Lu, Y. Spectroscopic and Computational Study of a Nonheme Iron Nitrosyl Center in a Biosynthetic Model of Nitric Oxide Reductase. *Angew. Chem. Int. Ed.* **2014**, *53* (9), 2417–2421. DOI: 10.1002/anie.201308431.

(39) Chakraborty, S.; Reed, J.; Sage, J. T.; Branagan, N. C.; Petrik, I. D.; Miner, K. D.; Hu, M. Y.; Zhao, J.; Alp, E. E.; Lu, Y. Recent Advances in Biosynthetic Modeling of Nitric Oxide Reductases and Insights Gained from Nuclear Resonance Vibrational and Other Spectroscopic Studies. *Inorg. Chem.* **2015**, *54* (19), 9317–9329. DOI: 10.1021/acs.inorgchem.5b01105.

(40) Hwang, H. J.; Carey, J. R.; Brower, E. T.; Gengenbach, A. J.; Abramite, J. A.; Lu, Y. Blue Ferrocenium Azurin: An Organometallopeptide with Tunable Redox Properties. *J. Am. Chem. Soc.* **2005**, *127* (44), 15356–15357. DOI: 10.1021/ja054983h.

(41) Ohashi, M.; Koshiyama, T.; Ueno, T.; Yanase, M.; Fujii, H.; Watanabe, Y. Preparation of Artificial Metalloenzymes by Insertion of Chromium(III) Schiff Base Complexes into Apomyoglobin Mutants. *Angewandte Chemie International Edition* **2003**, *42* (9), 1005–1008. DOI: 10.1002/anie.200390256.

(42) Carey, J. R.; Ma, S. K.; Pfister, T. D.; Garner, D. K.; Kim, H. K.; Abramite, J. A.; Wang, Z.; Guo, Z.; Lu, Y. A Site-Selective Dual Anchoring Strategy for Artificial Metallopeptide Design. *J. Am. Chem. Soc.* **2004**, *126* (35), 10812–10813. DOI: 10.1021/ja046908x.

(43) Garner, D. K.; Liang, L.; Barrios, D. A.; Zhang, J.-L.; Lu, Y. The Important Role of Covalent Anchor Positions in Tuning Catalytic Properties of a Rationally Designed MnSalen-Containing Metalloenzyme. *ACS Catal.* **2011**, *1* (9), 1083–1089. DOI: 10.1021/cs200258e.

(44) Zhang, J.-L.; Garner, D. K.; Liang, L.; Chen, Q.; Lu, Y. Protein Scaffold of a Designed Metalloenzyme Enhances the Chemoselectivity in Sulfoxidation of Thioanisole. *Chem. Commun.* **2008**, *0* (14), 1665–1667. DOI: 10.1039/B718915J.

(45) Oohora, K.; Meichin, H.; Kihira, Y.; Sugimoto, H.; Shiro, Y.; Hayashi, T. Manganese(V) Porphycene Complex Responsible for Inert C–H Bond Hydroxylation in a Myoglobin Matrix. *J. Am. Chem. Soc.* **2017**, *139* (51), 18460–18463. DOI: 10.1021/jacs.7b11288.

(46) McLaughlin, M. P.; Retegan, M.; Bill, E.; Payne, T. M.; Shafaat, H. S.; Peña, S.; Sudhamsu, J.; Ensign, A. A.; Crane, B. R.; Neese, F.; Holland, P. L. Azurin as a Protein Scaffold for a Low-Coordinate Nonheme Iron Site with a Small-Molecule Binding Pocket. *J. Am. Chem. Soc.* **2012**, *134* (48), 19746–19757. DOI: 10.1021/ja308346b.

(47) Liu, J.; Meier, K. K.; Tian, S.; Zhang, J.; Guo, H.; Schulz, C. E.; Robinson, H.; Nilges, M. J.; Münck, E.; Lu, Y. Redesigning the Blue Copper Azurin into a Redox-Active Mononuclear Nonheme Iron Protein: Preparation and Study of Fe(II)-M121E Azurin. *J. Am. Chem. Soc.* **2014**, *136* (35), 12337–12344. DOI: 10.1021/ja505410u.

(48) Manesis, A. C.; Shafaat, H. S. Electrochemical, Spectroscopic, and Density Functional Theory Characterization of Redox Activity in Nickel-Substituted Azurin: A Model for Acetyl-CoA Synthase. *Inorg. Chem.* **2015**, *54* (16), 7959–7967. DOI: 10.1021/acs.inorgchem.5b01103.

(49) Manesis, A. C.; O'Connor, M. J.; Schneider, C. R.; Shafaat, H. S. Multielectron Chemistry within a Model Nickel Metalloprotein: Mechanistic Implications for Acetyl-CoA Synthase. *J. Am. Chem. Soc.* **2017**, *139* (30), 10328–10338. DOI: 10.1021/jacs.7b03892.

(50) Slater, J. W.; Shafaat, H. S. Nickel-Substituted Rubredoxin as a Minimal Enzyme Model for Hydrogenase. *J. Phys. Chem. Lett.* **2015**, *6* (18), 3731–3736. DOI: 10.1021/acs.jpclett.5b01750.

(51) Stevenson, M. J.; Marguet, S. C.; Schneider, C. R.; Shafaat, H. S. Light-Driven Hydrogen Evolution by Nickel-Substituted Rubredoxin. *ChemSusChem* **2017**, *10* (22), 4424–4429. DOI: 10.1002/cssc.201701627.

(52) Slater, J. W.; Marguet, S. C.; Cirino, S. L.; Maugeri, P. T.; Shafaat, H. S. Experimental and DFT Investigations Reveal the Influence of the Outer Coordination Sphere on the Vibrational Spectra of Nickel-Substituted Rubredoxin, a Model Hydrogenase Enzyme. *Inorg. Chem.* **2017**, *56* (7), 3926–3938. DOI: 10.1021/acs.inorgchem.6b02934.

(53) Slater, J. W.; Marguet, S. C.; Monaco, H. A.; Shafaat, H. S. Going beyond Structure: Nickel-Substituted Rubredoxin as a Mechanistic Model for the [NiFe] Hydrogenases. *J. Am. Chem. Soc.* **2018**, *140* (32), 10250–10262. DOI: 10.1021/jacs.8b05194.

(54) Sigman, J. A.; Kim, H. K.; Zhao, X.; Carey, J. R.; Lu, Y. The Role of Copper and Protons in Heme-Copper Oxidases: Kinetic Study of an Engineered Heme-Copper Center in Myoglobin. *PNAS* **2003**, *100* (7), 3629–3634. DOI: 10.1073/pnas.0737308100.

(55) Bhagi-Damodaran, A.; Michael, M. A.; Zhu, Q.; Reed, J.; Sandoval, B. A.; Mirts, E. N.; Chakraborty, S.; Moënne-Locoz, P.; Zhang, Y.; Lu, Y. Why Copper Is Preferred over Iron for Oxygen Activation and Reduction in Haem-Copper Oxidases. *Nat. Chem.* **2017**, *9* (3), 257–263. DOI: 10.1038/nchem.2643.

(56) Reed, J. H.; Shi, Y.; Zhu, Q.; Chakraborty, S.; Mirts, E. N.; Petrik, I. D.; Bhagi-Damodaran, A.; Ross, M.; Moënne-Locoz, P.; Zhang, Y.; Lu, Y. Manganese and Cobalt in the Nonheme-Metal-Binding Site of a Biosynthetic Model of Heme-Copper Oxidase Superfamily Confer Oxidase Activity through Redox-Inactive Mechanism. *J. Am. Chem. Soc.* **2017**, *139* (35), 12209–12218. DOI: 10.1021/jacs.7b05800.

(57) Sabuncu, S.; Reed, J. H.; Lu, Y.; Moënne-Locoz, P. Nitric Oxide Reductase Activity in Heme–Nonheme Binuclear Engineered Myoglobins through a One-Electron Reduction Cycle. *J. Am. Chem. Soc.* **2018**, *140* (50), 17389–17393. DOI: 10.1021/jacs.8b11037.